CHAPTER 15

ANALYSIS OF PILE GROUPS

15.1 INTRODUCTION

Two general problems must be addressed in the analysis of pile groups: computation of the loads coming to each pile in the group and determination of the efficiency of a group of closely spaced piles. Both of these problems are important components in the area of soil–structure interaction. If piles are far apart in terms of multiples of pile diameter, pile–soil–pile interaction will not occur. As the piles become closer to each other, the stress in the soil from the distribution of axial load or lateral load to the soil will affect nearby piles. The simple way to consider the influence of the effect of the stresses in the soil is to think of the efficiency of closely spaced piles becoming less than unity. Methods of predicting efficiency will be discussed here.

15.2 DISTRIBUTION OF LOAD TO PILES IN A GROUP: THE TWO-DIMENSIONAL PROBLEM

The problem of solving for the distribution of axial and lateral loads to each pile in a group has long been of concern to geotechnical engineers, and various concepts have been proposed to find a solution. As the ideas of soil–structure interaction were developed, allowing the movements of pile heads to be computed for axial and lateral loading, it became possible to develop fully rational solutions to the problem of distribution of loading to piles in a group. The work of Hrennikoff (1950), based on linear analysis, provided an excellent guideline to the nonlinear problem. Useful information can be ob-

tained by considering the piles as behaving in a linear fashion, but the actual behavior of a system can be found only by finding the loading that causes failure. This requires the analysis to be continued well into the nonlinear response of the piles to loading, either axial or lateral. Failure may occur in the analysis due to the computation of a plastic hinge in one of the piles in a group or due to excessive deflection. The ability to determine the movement of a group of piles if a nonlinear response of a single pile is considered, due to axial or lateral loading, allows the engineer to design a group of piles for superstructures with a wide range of tolerances to foundation movements.

The response of a group of piles is analyzed for two conditions; the first is where loading is symmetrical about the line of action of the lateral load. That is, no twisting of the pile group will occur, so no pile is subjected to torsion. Therefore, each pile in the group can undergo two translations and a rotation, the two-dimensional problem. However, the method can also be extended to the general case where each pile can undergo three translations and three rotations (Robertson, 1961; Reese et al., 1970; Bryant, 1977; O'Neill, et al., 1977).

The analyses presented in this section assume that the soil does not act against the pile cap. In many instances, of course, the pile cap is cast against the soil. With regard to lateral resistance, shrinkage of the soil could cause a gap between concrete and soil. A small settlement of the ground surface would eliminate most of the vertical resistance against the mat. A conservative assumption is that the piles under the pile cap support the total load on the structure. In some current designs, however, the vertical loading is resisted by both a mat (raft) and by piles, termed a *piled raft* (Franke, 1991; El-Mossallamy and Franke, 1997). The analysis of a piled raft requires the development of an appropriate model for the entire system of raft, piles, and supporting soil.

The derivation of the equations presented here is based on the assumption that the piles are spaced far enough apart that there is no loss of efficiency; thus, the distribution of stress and deformation from a given pile to other piles in the group need not be considered. The method that is derived can be used with a group of closely spaced piles, but another level of iteration will be required.

15.2.1 Model of the Problem

The problem to be solved is shown in Figure 15.1. Three piles supporting a pile cap are shown. The piles may be of any size and placed on any batter, and may have any penetration below the groundline. The bent may be supported by any number of piles, but the piles are assumed to be far enough apart that each is 100% efficient. The soil and loading may have any characteristics for which the response of a single pile may be computed.

The derivation of the necessary equations in general form proceeds conveniently from the consideration of a structure such as that shown in Figure 15.2 (Reese, 1966; Reese and Matlock, 1966). The sign conventions for the

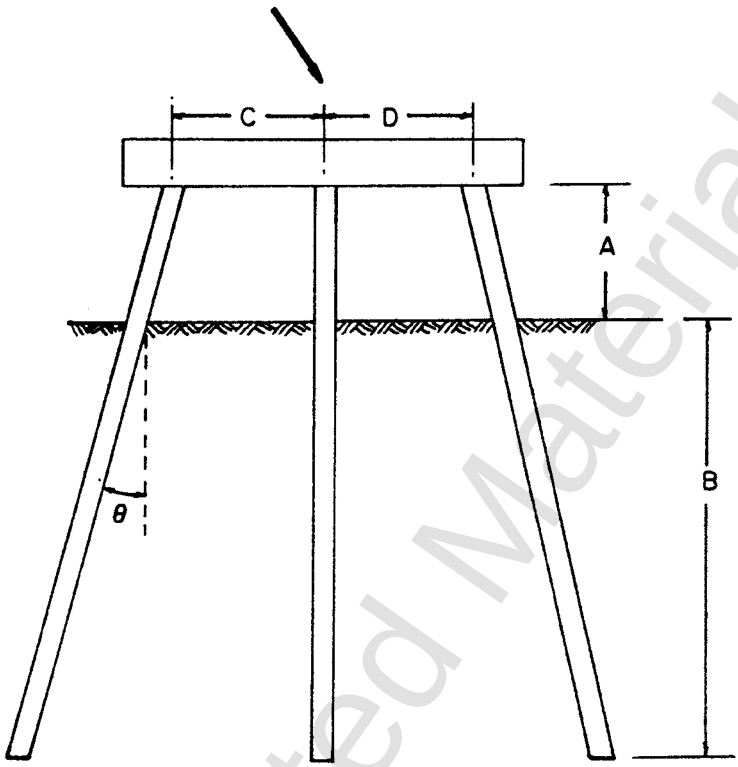

Figure 15.1 Example problem to be solved for the distribution of loads to piles in a group.

loading and the geometry are shown. A global coordinate system, *a*-*b*, is established with reference to the structure. A coordinate system, *x*-*y*, is established for each pile. For convenience in deriving the equilibrium equations, the *a*-*b* axes are located so that all of the coordinates of the pile heads are positive.

The soil is not shown, and the piles are replaced with a set of *springs* (mechanisms) that represent the interaction between the piles and the supporting soil (Figure 15.2). If the global coordinate system translates horizontally Δh and vertically Δv and rotates through the angle α_s, the movement of the head of each pile can be readily found. The angle α_s is assumed to be small in the derivation.

The movement of a pile head x_i in the direction of the axis of the pile is

$$x_t = (\Delta h + b\alpha_s)\sin\theta + (\Delta v + a\alpha_s)\cos\theta \tag{15.1}$$

The movement of a pile head y_t transverse to the direction of the axis of the pile (the lateral deflection) is

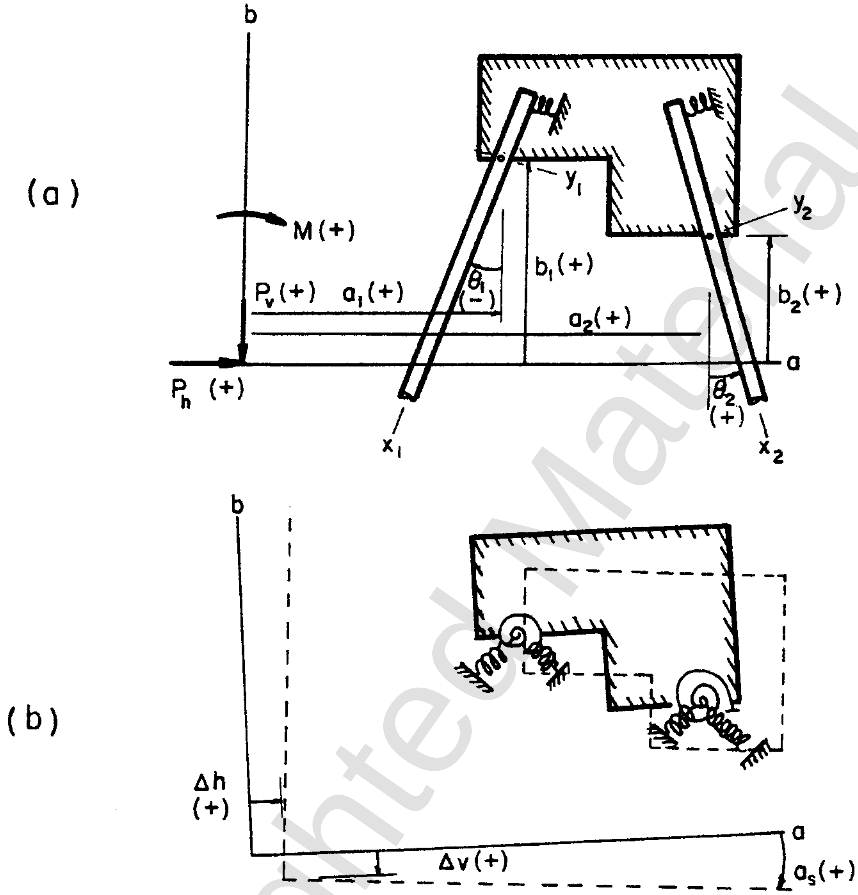

Figure 15.2 Model for the problem of distribution of loads to piles in a group.

$$y_t = (\Delta h + b\alpha_s)\cos\theta - (\Delta v + a\alpha_s)\sin\theta \tag{15.2}$$

The assumption made in deriving Eqs. 15.1 and 15.2 is that the pile heads have the same relative positions in space before and after loading. However, if the pile heads move relative to each other, an adjustment can be made in Eqs. 15.1 and 15.2 and a solution achieved by iteration.

The movements computed by Eqs. 15.1 and 15.2 will generate forces and moments at the pile head. The assumption is made that curves can be developed, usually nonlinear, that give the relationship between pile-head movement and pile-head forces. A secant to a curve is obtained and called the *modulus of pile-head resistance.* The values of the moduli, so obtained, can then be used, as shown below, to compute the components of movement of

the structure. If the values of the moduli that were selected were incorrect, iterations are made until convergence is obtained.

Using sign conventions established for the single pile under lateral loading, the lateral force P_t at the pile head is defined as follows:

$$P_t = J_y y_t \tag{15.3}$$

If rotational restraint exists at the pile head, the moment is

$$M_s = -J_m y_t \tag{15.4}$$

The moduli J_y and J_m are not single-valued functions of pile-head translation but are also functions of the rotation α_s of the structure. Figures 15.1 and 15.2 indicate that some of the piles supporting a structure may be installed on a batter. The next section presents an empirical but effective procedure for making the required modifications if some of the piles in a structure are battered.

If it is assumed that a compressive load causes a positive deflection along the pile axis, the axial force P_x may be defined as follows:

$$P_x = J_x x_t \tag{15.5}$$

A pile under lateral loading will almost always experience a lateral deflection at the groundline that could cause some loss of axial capacity. However, the loss would be small, so P_x can be taken as a single-valued function of x_t.

A curve showing axial load versus deflection may be computed by one of the procedures recommended by several authors (Reese, 1964; Coyle and Reese, 1966; Coyle and Sulaiman, 1967; Kraft et al., 1981) in Chapter 13 or the results from a field load test may be used. A typical curve is shown in Figure 15.3a. The curve is shown in the first quadrant for convenience in plotting, but under some loadings, one or more of the piles in a structure may be subjected to uplift and a curve showing axial load in tension must be computed.

The methods for computing the response of a pile under lateral loading by computer have been presented in Chapter 14 and may easily be employed for computing the curves shown in Figures 15.3b and 15.3c. The method used to attach the piles to the superstructure must be taken into account because the pile-head rotation α_p will be affected. Also, if the pile heads are fully or partially restrained against rotation, the rotation of the structure α_s will affect the curves in Figures 15.3b and 15.3c. Alternatively, the nondimensional methods presented earlier in Chapter 12 may be used in obtaining the curves for the response of the pile to lateral loading.

The forces at the pile head defined in Eqs. 15.3 through 15.5 may now be resolved into vertical and horizontal components of force on the structure as follows:

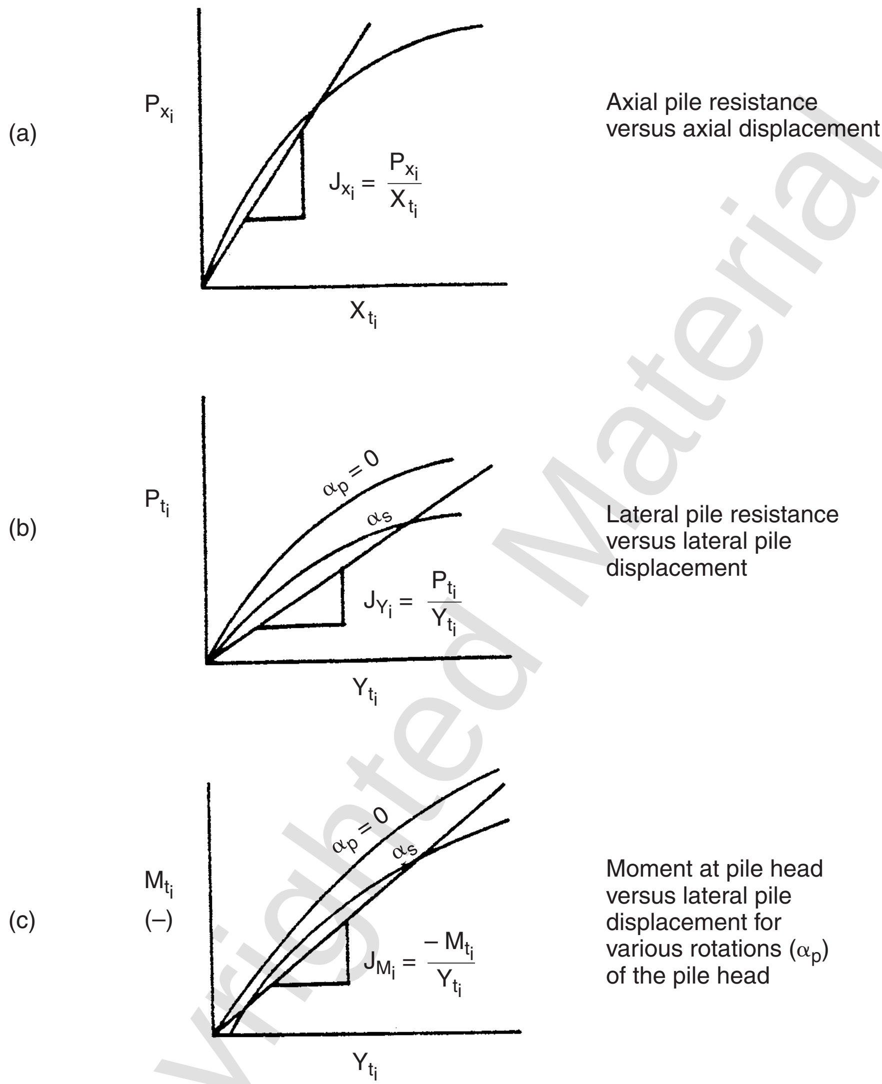

Figure 15.3 Typical curves showing pile resistance as a function of deflection for a pile in a group.

$$F_v = -(P_x \cos\theta - P_t \sin\theta) \tag{15.6}$$

$$F_h = -(P_x \sin\theta + P_t \cos\theta) \tag{15.7}$$

The moment on the structure is

$$M_s = J_m y_t \tag{15.8}$$

The equilibrium equations can now be written as follows:

$$P_v + \sum F_{v_i} = 0 \tag{15.9}$$

$$P_h + \sum F_{h_i} = 0 \tag{15.10}$$

$$M + \sum M_{s_i} + \sum a_i F_{v_i} + \sum b_i F_{h_i} = 0 \tag{15.11}$$

The subscript *i* refers to values of any "*i*th" pile. Using Eqs. 15.1 through 15.8, Eqs. 15.9 through 15.11 may be written in terms of the structural movements as shown in Eqs. 15.12 through 15.14.

$$\Delta v\left[\sum A_i\right] + \Delta h\left[\sum B_i\right] + \alpha_s\left[\sum a_i A_i + \sum b_i B_i\right] = P_v \tag{15.12}$$

$$\Delta v\left[\sum B_i\right] + \Delta h\left[\sum C_i\right] + \alpha_s\left[\sum a_i B_i + \sum b_i C_i\right] = P_h \tag{15.13}$$

$$\begin{aligned}\Delta v&\left[\sum D_i + \sum a_i A_i + \sum b_i B_i\right] + \Delta h\left[\sum E_i + \sum a_i B_i + \sum b_i C_i\right] \\ &+ \alpha_s\left[\sum a_i D_i + \sum a_i^2 A_i + \sum b_i E_i + \sum b_i^2 C_i + \sum 2a_i b_i B_i\right] = M\end{aligned} \tag{15.14}$$

where

$$A_i = J_{x_i} \cos^2 \theta_i + J_{y_i} \sin^2 \theta_i \tag{15.15}$$

$$B_i = (J_{x_i} - J_{y_i})\sin \theta_i \cos \theta_i \tag{15.16}$$

$$C_i = J_{x_i} \sin^2 \theta_i + J_{y_i} \cos^2 \theta_i \tag{15.17}$$

$$D_i = J_{m_i} \sin \theta_i \tag{15.18}$$

$$E_i = -J_{m_i} \cos \theta_i \tag{15.19}$$

The above equations are not as complex as they appear. For example, the origin of the coordinate system can usually be selected so that all of the *b*-values are zero. For vertical piles, the sine terms are zero and the cosine terms are unity. For small deflections, the *J*-values can all be taken as constants. Therefore, under many circumstances, it is possible to solve the above equations by hand. However, if the deflections of the group are such that the

nonlinear portion of the curves in Figure 15.3 is reached, a computer solution is advantageous. Computer solutions are discussed later in this chapter.

15.2.2 Detailed Step-by-Step Solution Procedure

1. Study the foundation to be analyzed and select a two-dimensional bent the behavior of which is representative of the entire system.
2. Prepare a sketch such that the lateral loading comes from the left. Show all pertinent dimensions.
3. Select a coordinate center and find the horizontal component of load, the vertical component of load, and the moment through and about that point.
4. Compute a curve showing axial load versus axial deflection for each pile in the group or, preferably, use the results from a field load test. Computation of a curve showing axial load versus settlement is presented in detail in Chapter 13.
5. Compute curves showing lateral load as a function of lateral deflection and moment as a function of lateral deflection, taking into account the effect of structural rotation on the boundary conditions at each pile head.
6. Estimate trial values of J_x, J_y, and J_m for each pile in the structure.
7. Solve Eqs. 15.12 through 15.14 for values of Δv, Δh, and α_s.
8. Compute movements of pile heads, obtain loads at pile heads by use of the appropriate J-values, and check to ensure that equilibrium was established for the group.
9. If necessary, obtain new values of J_x, J_y, and J_m for each pile and solve Eqs. 15.12 through 15.14 again for the new values of Δv, Δh, and α_s.
10. Continue iteration until the computed values of the structural movements agree, within a given tolerance, with the values from the previous computation.
11. Compute the stresses along the length of each pile using the loads and moments at each pile head.

15.3 MODIFICATION OF *p-y* CURVES FOR BATTERED PILES

Kubo (1965) and Awoshika and Reese (1971) investigated the effect of batter on the behavior of laterally loaded piles. Kubo used model tests in sands and full-scale field experiments to obtain his results. Awoshika and Reese tested 2-in.-diameter piles in sand. The value of the constant showing the increase or decrease in soil resistance as a function of the angle of batter may be obtained for the line in Figure 15.4. The ratio of soil resistance was obtained

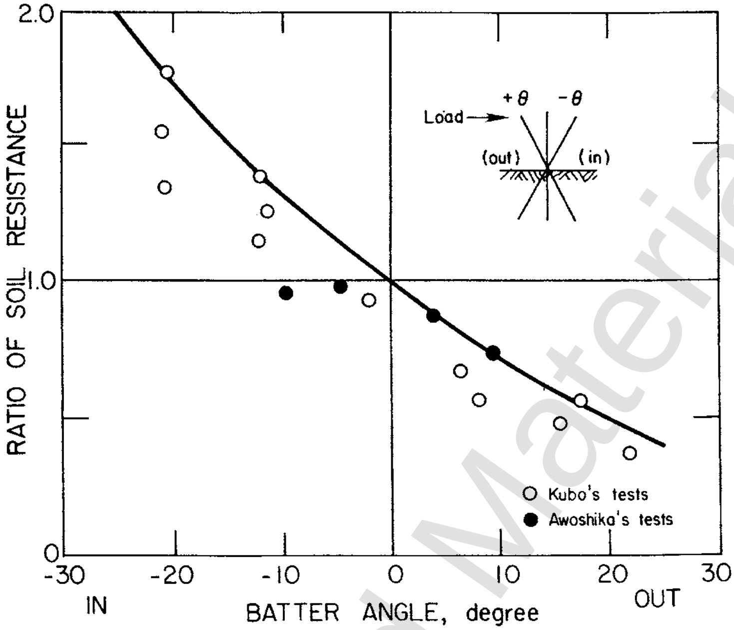

Figure 15.4 Experimental results showing loss of resistance as a function of batter angle for battered piles.

by comparing the groundline deflection for a battered pile with that of a vertical pile and is, of course, based purely on experiment.

The correction for batter is made as follows: (1) enter Figure 15.4 with the angle of batter, positive or negative, and obtain a value of the ratio; (2) compute groundline deflection as if the pile were vertical; (3) multiply the deflection found in (2) by the ratio found in (1); (4) vary the strength of the soil until the deflection found in (3) is obtained; and (5) use the modified strength found in (4) for the further computations of the behavior of the pile on a batter. The method outlined is obviously approximate and should be used with caution. If the project is large and expensive, field tests on piles that are battered and vertical could be justified.

15.4 EXAMPLE SOLUTION SHOWING DISTRIBUTION OF A LOAD TO PILES IN A TWO-DIMENSIONAL GROUP

15.4.1 Solution by Hand Computations

The detailed step-by-step procedure was presented earlier and is followed in the following example. Steps 1 through 3 were followed in preparing Figure 15.5. The pile-supported retaining wall has piles spaced 8 ft apart along the

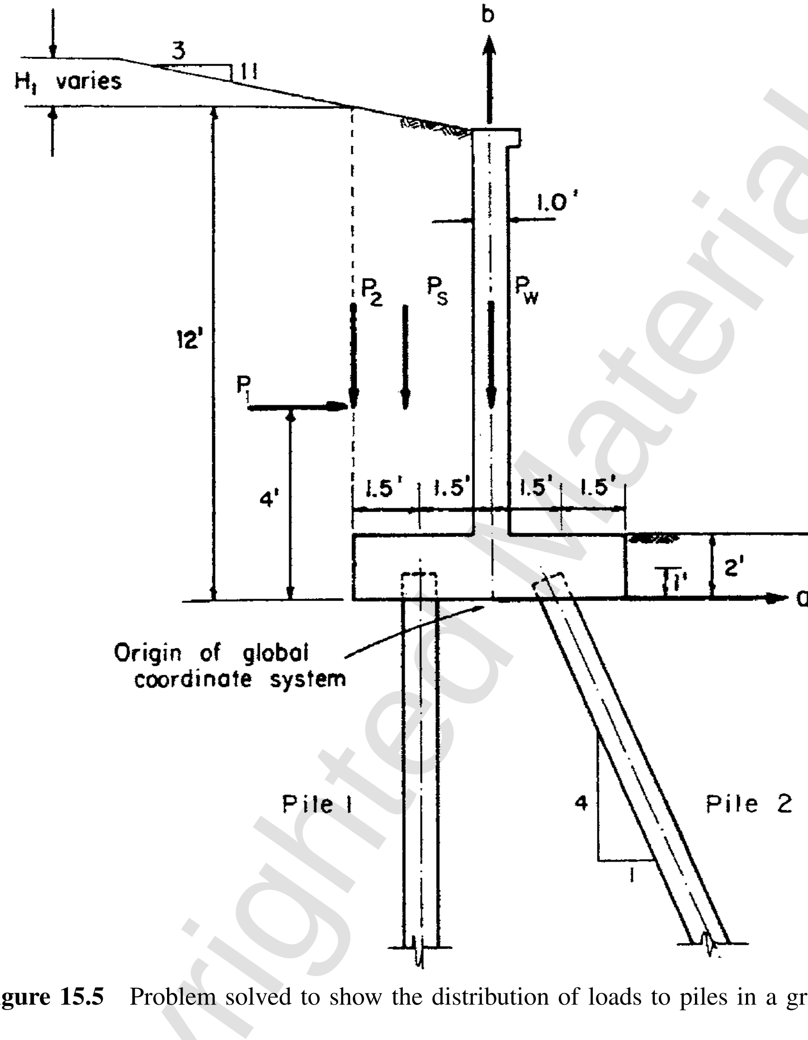

Figure 15.5 Problem solved to show the distribution of loads to piles in a group.

wall. The piles are steel pipes, 12 in. in outside diameter with a wall thickness of 0.5 in. The length of the piles is 40 ft. As shown in the figure, the piles are embedded only 1 ft. in the cap, and the assumption is made that the pile heads are unrestrained against rotation. This condition generally does not exist; if a pile is embedded a sufficient amount to sustain shear, some restraint against rotation must occur. Consideration of the effect of some rotational restraint shows that the assumption that the pile can rotate freely adds a small degree of safety to the solution.

The backfill is a free-draining granular soil without any fine particles. The surface of the backfill is treated to facilitate runoff, and weep holes are provided so that water will not collect behind the wall. The soil supporting the piles is a silty clay, with the water table reported as having a depth of 10 ft.

The water content averages 10% above and 20% below the water table. The undrained shear strength of the clay varies with depth, and a constant value of 2.0 kips/ft^2 was selected for the analyses. The unit weight of the clay is 118 lb/ft^3 above the water table, and a value of ε_{50} was estimated to be 0.005.

The pile to the right in the figure was battered at an angle of 14° with the vertical such that the soil resistance would be less than for a vertical pile. Figure 15.4 was employed, and a soil resistance ratio of 0.62 was found. Therefore, the soil strength around the battered pile was taken as (0.62)(2.0) = 1.24 kips/ft^2.

The forces P_1, P_2, P_s, and P_w (shown in Figure 15.5) were computed as to be: 21.4, 4.6, 18.4, and 22.5 kips, respectively. Resolution of the loads at the origin of the global coordinate system resulted in the following service loads: P_v = 45.5 kips, P_h = 21.4 kips, and M = 44.2 ft-kips. The value of the moment of inertia I of the pile is 299 in.^{4}. The yield strength of the steel is 36 kips/in.^{2}.

With regard to Step 4, a field load test was assumed at the site and the ultimate axial capacity of a pile was found to be 240 kips. The load-settlement curve is shown in Figure 15.6. Step 5 was accomplished by computing a set of *p-y* curves for Pile 1, the vertical pile, and for Pile 2, the battered pile, and shown in Figures 15.7 and 15.8. In complying with Step 5, with the sets of *p-y* curves, the curves showing lateral load versus deflection for the tops of Piles 1 and 2 may be developed by using the nondimensional curves demonstrated earlier. However, a computer solution was employed as described in Chapter 14, and the results are shown in Figures 15.9 and 15.10 for Piles 1 and 2, respectively. The figures do not indicate an influence of α_s, the rotation of the structure, because the heads of the piles are unrestrained against rotation.

Step 6 was accomplished by assuming that the movements of the pile heads would be small for the service loads indicated in Figure 15.5. The *J*-values were found by obtaining the slopes of the curves in Figures 15.6, 15.8, and 15.9 to the first points shown in the figures, with the following results: J_{x_1} and J_{x_2} = 2800 kips/in., J_{y_1} = 333 kips/in., and J_{y_2} = 161 kips/in.

Substitution of the *J*-values into Eqs. 15.15 through 15.19, with the value of θ as 14°, yields the following values: A_1 = 2800.0, A_2 = 2645.5, B_1 = 0, B_2 = 619.46, C_1 = 333.00, C_2 = 315.45, and the remainder of the terms in the equations have values of zero.

Step 7 is to substitute these values into Eqs. 15.12 through 15.14 to obtain equations for the movement of the global coordinate system. The results for the service loadings on the structure are as follows:

$$\Delta v[5445.5] + \Delta h[619.46] + \alpha_s[-2781] = 45.5 \text{ k}$$

$$\Delta v[619.46] + \Delta h[618.45] + \alpha_s[11150] = 21.4 \text{ k}$$

$$\Delta v[-2781] + \Delta h[11150] + \alpha_s[1,764,300] = 530 \text{ in.-k}$$

The three equations may be solved by hand with a little effort, but a spreadsheet solution is convenient, with the following results:

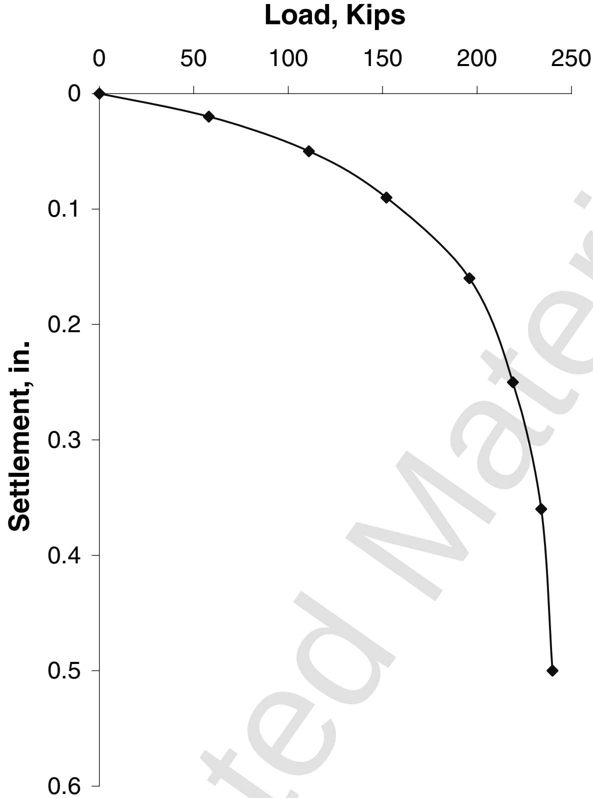

Figure 15.6 Axial load versus settlement for piles in the example problem.

$$\Delta v = 0.005579; \quad \Delta h = 0.025081; \quad \alpha_s = 0.000151$$

In Steps 8 through 10, the pile-head movements were computed with these movements of the global coordinate system, and the results from Eqs. 15.1 and 15.2 are as shown in the following table, along with the computed forces on the pile heads by use of the *J*-values assumed in the analysis.

Pile No.	x_t, in.	P_x, k	y_t, in.	P_t, k
1	0.002861	8.01	0.025081	8.35
2	0.014119	39.53	0.022329	3.59

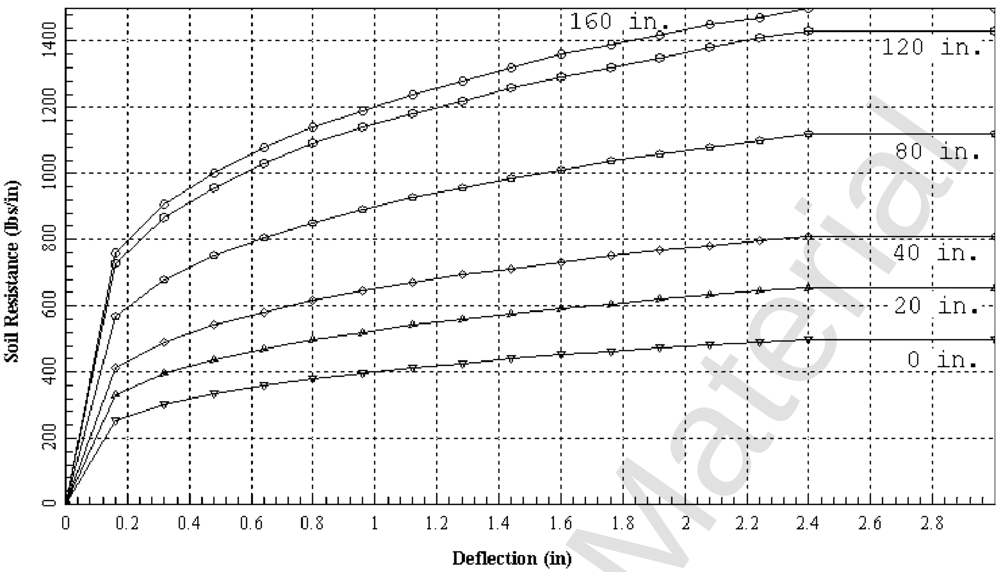

Figure 15.7 Curves showing soil resistance versus deflection (*p*-*y* curves) for vertical piles in the example problem.

The resisting loads on the pile cap generated by the pile-head movements show that the structure is in equilibrium; however, entering curves in Figures 15.6, 15.9, and 15.10 showed that the *J*-values had not been selected with sufficient accuracy. For example, entering Figure 15.9 with a pile-head deflection of 0.025081 yields a P_t of about 6 kips rather than 8.35 kips; thus, the *J*-values would need to be recomputed and a new solution obtained. This process or iteration requires the use of a computer. The GROUP program was employed, six iterations were required, and the following results were obtained:

Pile No.	x_t, in.	P_x, k	y_t, in.	P_t, k
1	0.00272	8.02	0.0321	7.05
2	0.0135	39.8	0.0298	4.83

As may be seen, the results were not very different, suggesting that useful solutions can be obtained by hand.

Step 11 will be demonstrated by using the results from a computer solution where the loadings were multiplied by a factor of 2.5, yielding P_v = 113,700

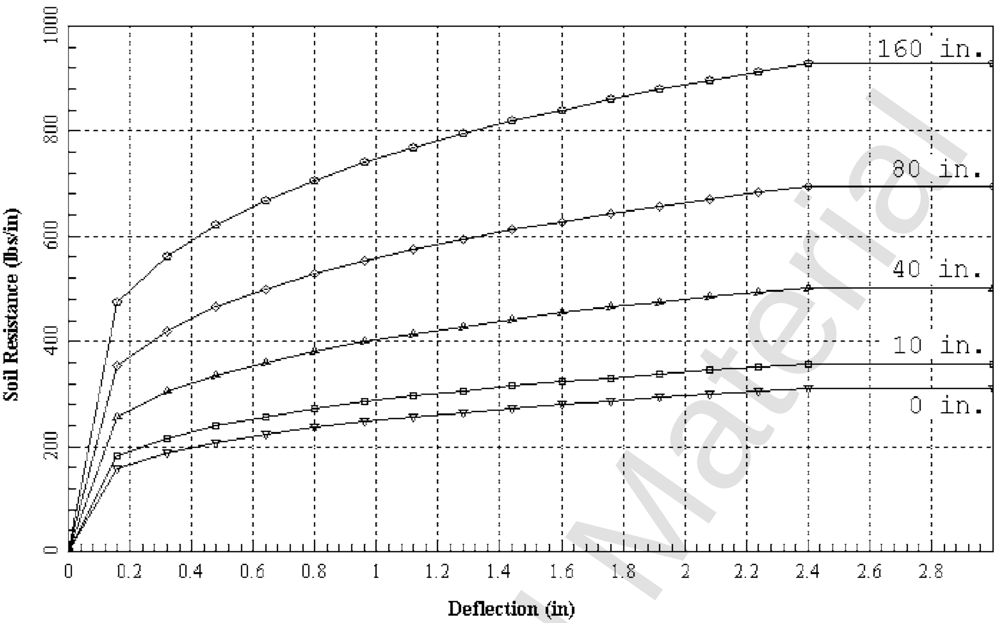

Figure 15.8 Curves showing soil resistance versus deflection (*p-y* curves) for batter piles in the example problem.

lb, P_h = 53,500 lb, and M = 1,325,000 in.-lb. The results for Piles 1 and 2 are as follows:

Pile No.	x_t, in.	P_x, k	y_t, in.	P_t, k	$f_{\max}$, ksi
1	0.00679	20.0	0.289	18.2	10.9
2	0.0429	99.5	0.287	11.6	12.0

The pile-head movements and the loads with a load factor of 2.5 are shown in the above table, and the pile-head loads are presented in Figure 15.11. The table shows the lateral deflection with the load factor to be about 0.25 in. and the maximum stress to be far less than would cause a failure of the pile. The maximum axial load of 99.5 kips is far less than the load to cause failure of the pile (see Figure 15.6).

The above example may be viewed as part of an iteration to determine the pile size and spacing for the retaining-wall problem. The engineer may modify the pile diameter, wall thickness, and penetration and reconsider the distance between pile groups along the wall. The construction cost is increased for the driving of batter piles; two vertical piles could be investigated, along with other factors that influence the design.

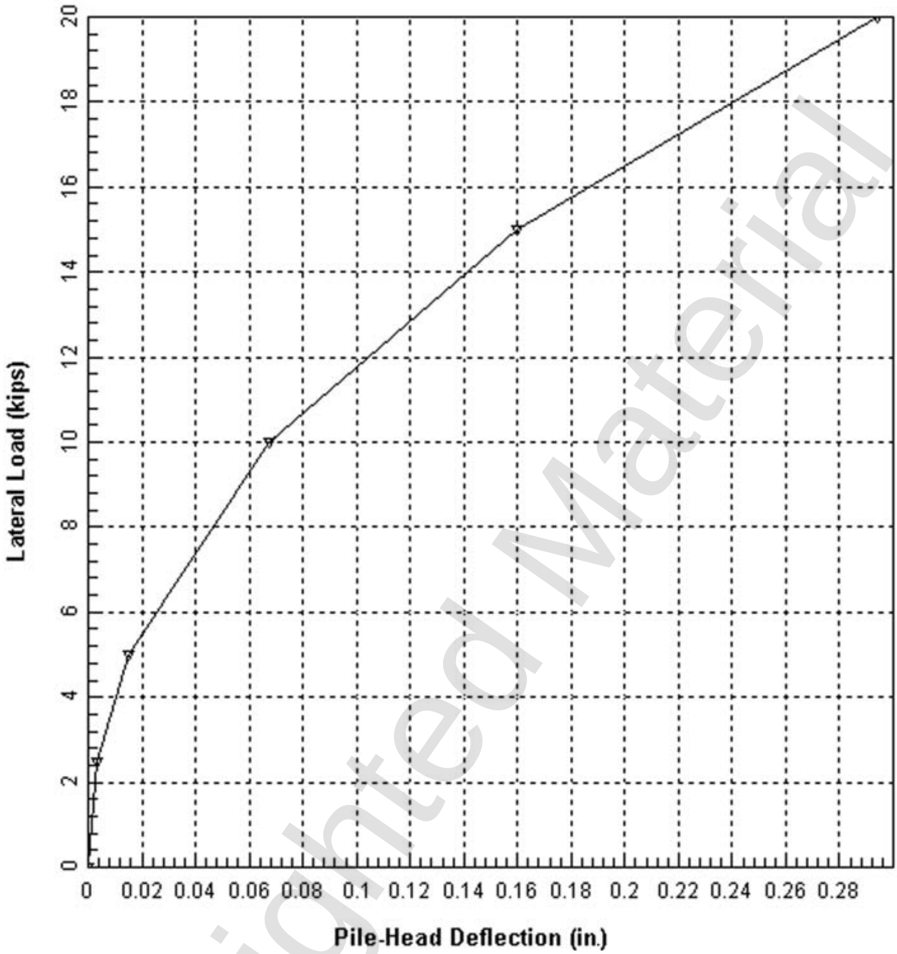

Figure 15.9 Lateral load versus deflection for pile head for vertical piles in the example problem.

15.5 EFFICIENCY OF PILES IN GROUPS UNDER LATERAL LOADING

15.5.1 Modifying Lateral Resistance of Closely Spaced Piles

O'Neill (1983) considered the response of a group of piles under both axial load and lateral load, and characterized the problem of closely spaced piles in a group as one of pile–soil–pile interaction. O'Neill listed a number of procedures that may be used in predicting the behavior of such groups. He states that none of the procedures should be expected to provide generally accurate predictions of the distribution of loads to piles in a group because none of the models account for installation effects. He concludes that more experimental data are needed. Sections 15.5.2 and 15.5.3 deal with lateral

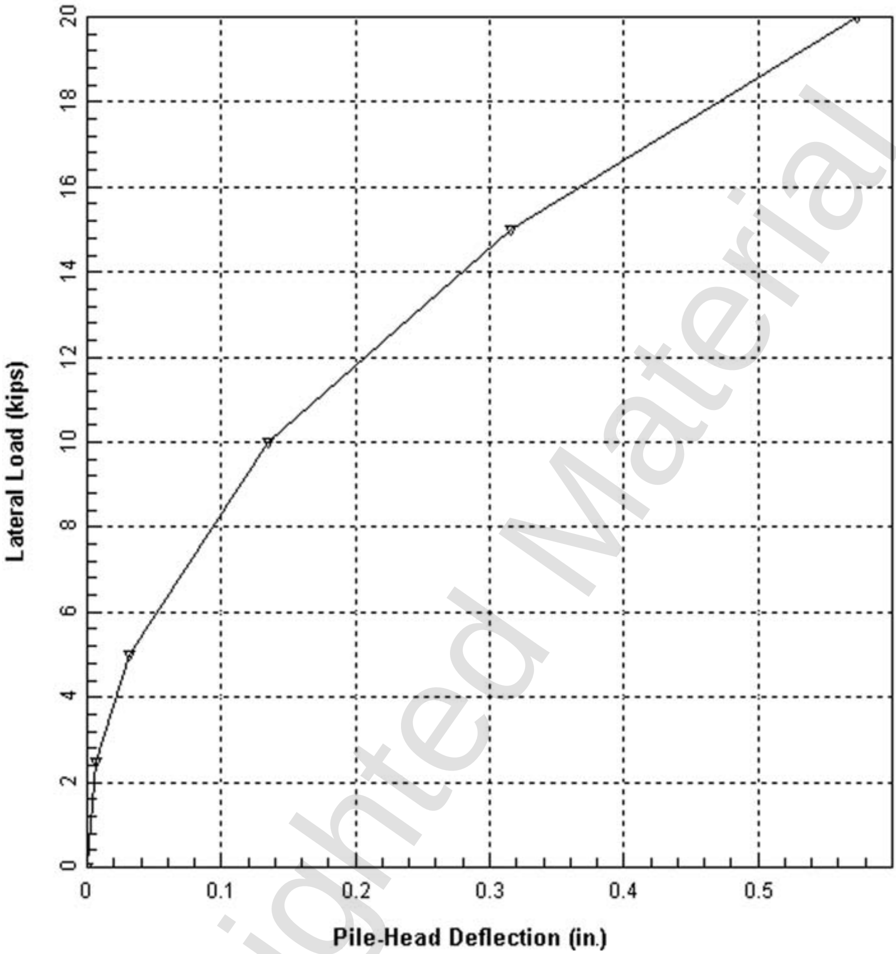

Figure 15.10 Lateral load versus deflection for pile head for batter piles in the example problem.

resistance. For the analysis of groups of piles, axial resistance must be modified for closely spaced piles. That topic was discussed in Section 15.6.

15.5.2 Customary Methods of Adjusting Lateral Resistance for Close Spacing

Pile–soil–pile interaction under close spacing is the reason that the piles in the group are less efficient than single piles. The theory of elasticity has been employed to take into account the effect of a single pile on other piles in the group. Solutions have been developed (Poulos, 1971; Banerjee and Davies,

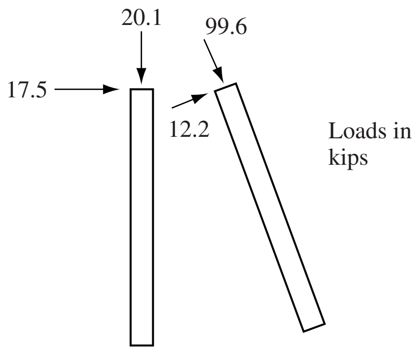

Figure 15.11 Loads at the pile heads for the example problem.

1979) that assume a linear response of the pile-soil system. While such methods are instructive, there is ample evidence to show that soils cannot generally be characterized as linear, homogeneous, elastic materials.

Two other approaches to the analysis of a group of closely spaced piles under lateral load are given in the following paragraphs. One method is to use a rather straightforward equation for the efficiency of piles in a group under lateral loading, such as Eq. 15.20; the other method is based on the assumption that the soil within the pile group moves laterally the same amount as the piles.

$$(Q_{\text{ult}})_G = En(Q_{\text{ult}})_p \tag{15.20}$$

where

$(Q_{\text{ult}})_G$ = ultimate lateral capacity of the group,
E = efficiency factor (1 or < 1),
n = number of piles in the group, and
$(Q_{\text{ult}})_p$ = ultimate lateral capacity of an individual pile.

Various proposals have been made for obtaining the value of E. For example, McClelland (1972) suggested that the value of E should be 1.0 for pile groups in cohesive soil with center-to-center spacing of eight diameters or more and that E should decrease linearly to 0.7 at a spacing of three diameters. McClelland based his recommendations on results from experiments in the field and in the laboratory. He did not differentiate between piles that are spaced front to back or side by side or spaced at some other angle between each other.

Unfortunately, experimental data on the behavior of pile groups under lateral load are limited. Furthermore, the mechanics of the behavior of a group of laterally loaded piles are more complex than those for a group of axially

loaded piles. Thus, few recommendations have been made for efficiency formulas for laterally loaded groups.

The single-pile method of analysis is based on the assumption that the soil between the piles moves with the group. Thus, the pile group with the contained soil can be treated as a single pile of large diameter.

A step-by-step procedure for using the method is as follows:

1. The group to be analyzed is selected, and a plan view of the piles at the groundline is prepared.
2. The minimum length is found for a line that encloses the group. If a nine-pile (3 by 3) group consists of piles that are one foot square and three widths on center, the length of the line will be 28 ft.
3. The length found in Step 2 is considered to be the circumference of a pile of large diameter; thus, the length is divided by π to obtain the diameter of the imaginary pile.
4. The next step is to determine the stiffness of the group. For a lateral load passing through the tops of the piles, the stiffness of the group is taken as the sum of the stiffnesses of the individual piles. Thus, it is assumed that the deflection at the pile top is the same for each pile in the group and, further, that the deflected shape of each pile is identical. Some judgment must be used if the piles in the group have different lengths.
5. Then an analysis is made for the imaginary pile, taking into account the nature of the loading and the boundary conditions at the pile head. The shear and moment for the imaginary large-sized pile are shared by the individual piles according to the ratio of the lateral stiffness of each pile to that of the group.

The shear, moment, pile-head deflection, and pile-head rotation yield a unique solution for each pile in the group. As a final step, it is necessary to compare the single-pile solution to that of the group. The piles in the group may have an efficiency greater than 1; in this case, the single-pile solutions would control.

An example problem is presented in Figure 15.12. The steel piles are embedded in a reinforced-concrete mat in such a way that the pile heads do not rotate. The piles are 14HP89 by 40 ft long and placed so that bending is about the strong axis. The moment of inertia is 904 in.^{4} and the modulus of elasticity is 30×10^6 lb/in.^{2}. The width of the section is 14.7 in. and the depth is 13.83 in.

The soil is assumed to be sand with an angle of internal friction of 34°, and the unit weight is 114 lb/ft^3. The computer program presented in Chapter 14 may be utilized. Alternatively, the *p-y* curves for the imaginary large-diameter pile could be prepared as described by Reese et al. (1974) or API (1987) and a solution developed using nondimensional curves. For a pile with

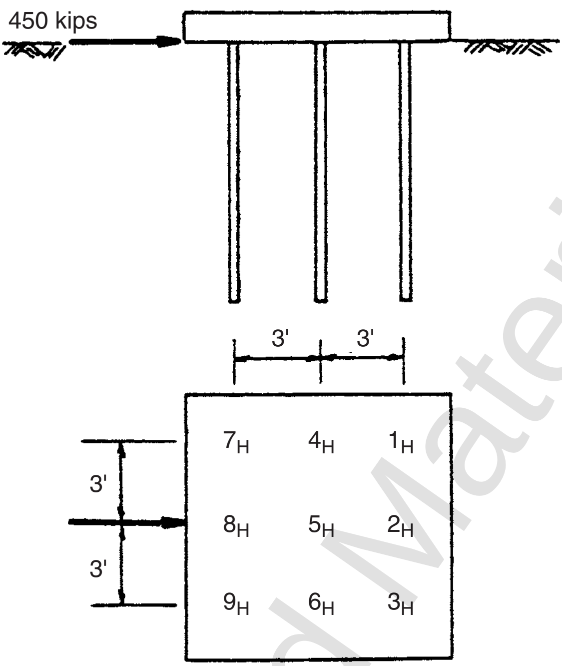

Figure 15.12 Example of a solution of the problem of closely spaced piles under lateral loading.

a diameter of 109.4 in. and a moment of inertia of 8136 in.^{4} (9 times 904), the results are as follows:

y_t = 0.885 in.
$M_t = M_{\max} = 3.60 \times 10^7$ in.-lb for group
Bending stress = 25.3 kips/in.^{2}

The deflection and stress are for a single pile of large diameter.

If a single pile with a diameter of 14.7 in. is analyzed with a load of 50 kips, the groundline deflection is 0.355 in. and the bending stress is 23.1 kips/in.^{2}. Therefore, the solution with the imaginary large-diameter single pile is more critical.

15.5.3 Adjusting for Close Spacing Under Lateral Loading by Modified *p-y* Curves

Bogard and Matlock (1983) present a method in which the *p-y* curves for a single pile are modified to take into account the group effect. Excellent agreement was obtained between their computed results and results from field

experiments (Matlock et al., 1980). Much of the detailed presentation that follows is based on the work of Brown et al. (1987), who tested single piles and groups under lateral loading, all instrumented for the measurement of bending moment with depth. Two major experiments were performed, in overconsolidated clay and in sand, and analyses showed that the group effect could be taken into account most favorably by reducing the value of p for the p-y curve of the single pile to obtain p-y curves for the pile group. The curves in Figure 15.13 show that the factor f_m may be used to reduce the values of p_{sp} for the single pile to the value p_{gp} for the pile group. The proposals make use of other work in the technical literature, some based on the results of model tests of pile groups (Prakash, 1962; Schmidt, 1981, 1985; Cox et al., 1984; Dunnavant and O'Neill, 1986; Wang, 1986; Lieng, 1988).

Side-By-Side Reduction Factors The first pattern for the placement of piles in a group to be considered is for piles placed side by side. Values of β are found, termed β_a for this case, and may be summed as shown later to determine a composite factor of β for each pile in the group. The pattern for the placement of the side-by-side piles is shown in Figure 15.14, with the arrows showing the direction of loading. The values of β_a may be found from the curve or equations given in Figure 15.14. The plotted points in the figure are identified by the references previously cited. The value of β_a may be taken directly from the plot or may be found by using the equation in the figure. As may be seen, with s/b values of 3.28 or more, the value of β_a is unity. The smallest value of β_a for piles that touch is 0.5. A review of the

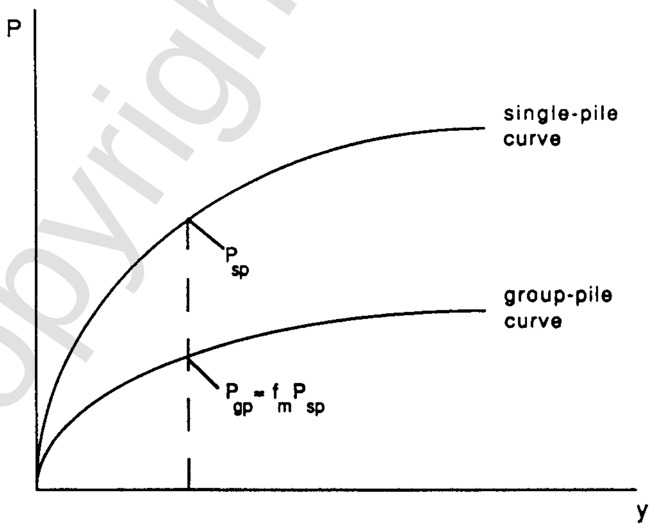

Figure 15.13 Employing a computed value of f_m to derive the p-y curve for piles in a group.

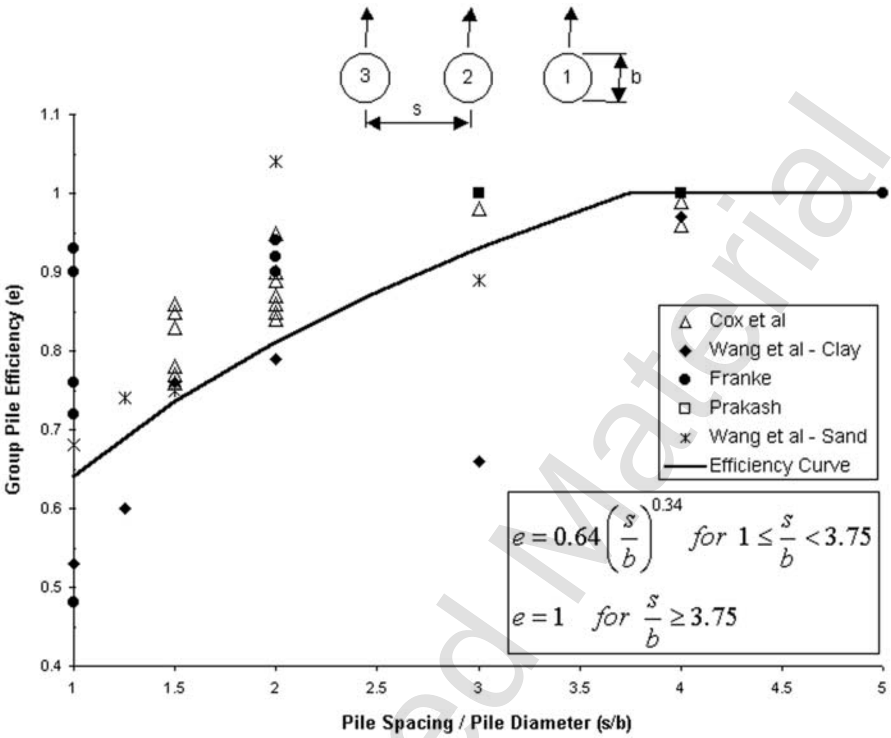

Figure 15.14 Curve giving reduction factors β_a for piles in a row.

plotted points reveals that the value of unity of β_a for s/b values of 3.28 or more is strongly supported. The value of 0.5 for piles that touch is found from mechanics. However, the first branch of the curve in Figure 15.14 is subject to uncertainty; this is not surprising, considering the variety of experiments that were cited.

Line-By-Line Reduction Factors, Leading Piles The next pattern of placement of the piles in a group to be considered is for piles placed in a line, as shown in Figure 15.15, with the arrow showing the direction of loading. The values of β_{bL} may be found from the curve or equations in Figure 15.15. The plotted points in the figure are identified by the references previously cited. The suggested curve agrees well with the plotted points except for four points to the left of the curve indicating an efficiency of unity for close spacing.

Line-By-Line Reduction Factors, Trailing Piles The experimental results, along with a suggested curve and equations, are given in Figure 15.16. The scatter of the plotted points indicates that the computed efficiency for the

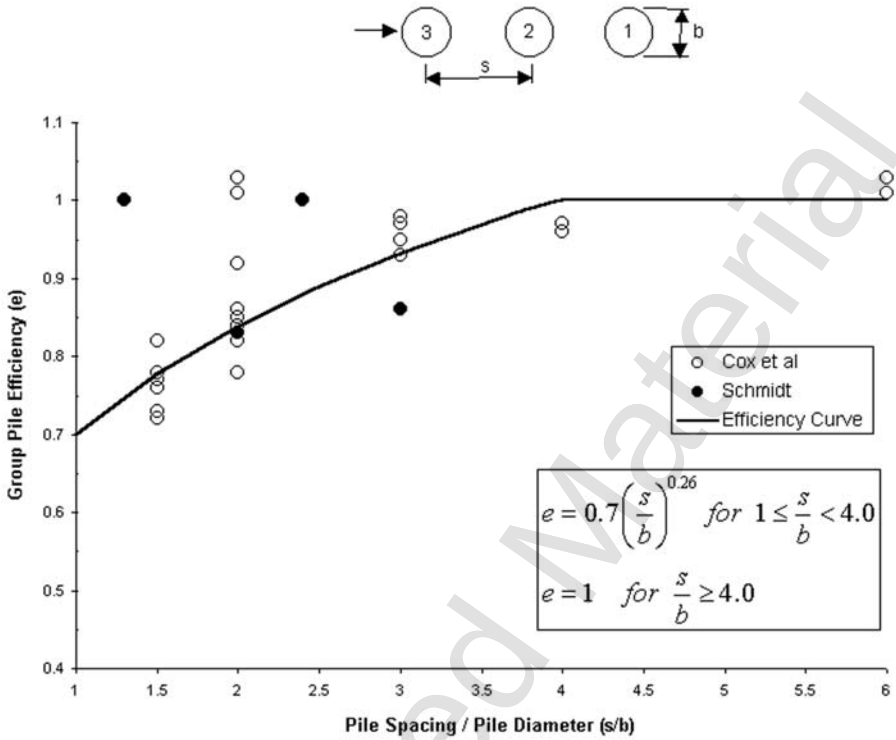

Figure 15.15 Curve giving reduction factors β_{bl} for leading piles in a line.

individual piles in a group is not likely to be precise. The scatter, as noted earlier, is not surprising in view of the many variables involved in the experiments. The authors maintain that the use of values suggested in the curves and equations in Figures 15.14 through 15.16 will yield a much better result than ignoring the effect of close spacing.

Skewed Piles The experiments cited above did not obtain data on skewed piles, but provision for skewed piles is necessary. A simple mathematical expression for the ellipse in polar coordinates was selected to obtain the reduction factor. The geometry of the two piles, A and B, is shown in Figure 15.17a. The side-by-side effect β_a may be found from Figure 15.14, where the spacing is r/b. The in-line effect β_b may be found from either Figure 15.16 or Figure 15.17, depending on whether Pile A or Pile B is being considered. The values of β_a and β_b are indicated in Figure 15.17b, and the value of β_s for the effect of skew may be found from the following equation:

$$\beta_s = (\beta_b^2 \cos^2 \phi + \beta_a^2 \sin^2 \phi)^{1/2} \tag{15.21}$$

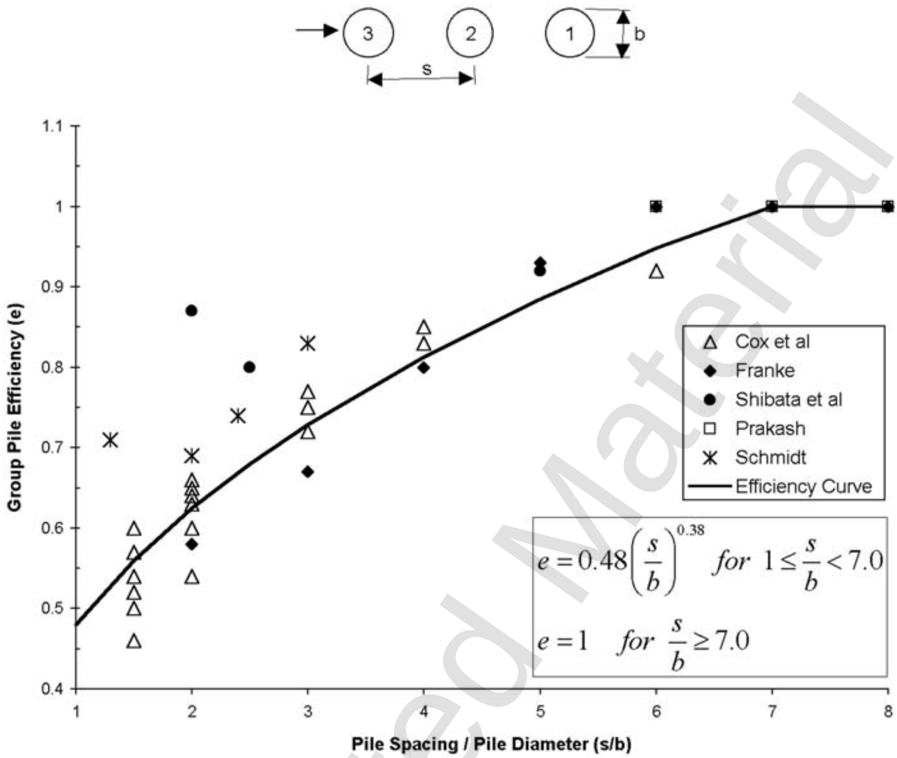

Figure 15.16 Curve giving reduction factors β_{bt} for trailing piles in a line.

Example Computation of Reduction Factors for Piles Under Lateral Loading The example selected for computation of the reduction factors for the group is presented in Figure 15.18. Pile 4 is selected as an example of the computation for each pile in the group. The value of f_m for Pile 4 to obtain the modified *p-y* curve for *that pile* in the group is obtained as follows:

$$
\begin{aligned}
f_{m4} = {} & \beta_{34} \quad \text{(side by side effect)} \\
& \times \beta_{24} \quad \text{(trailing effect)} \\
& \times \beta_{64} \quad \text{(leading effect)} \\
& \times \beta_{14} \quad \text{(skewed effect)} \\
& \times \beta_{54} \quad \text{(skewed effect)}
\end{aligned}
$$

Employing the information in Figures 15.14 through 15.16 and Eq. 15.21, the following values were computed:

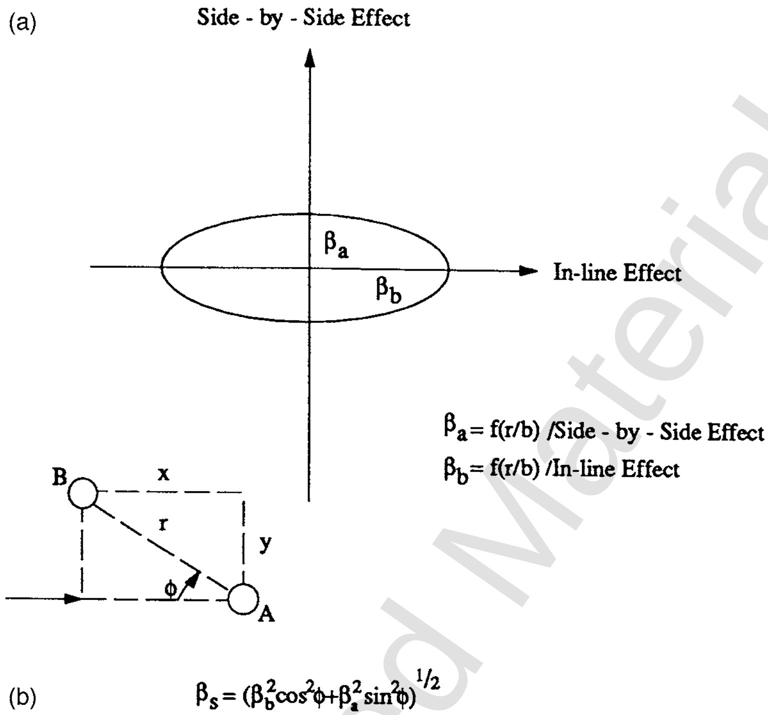

Figure 15.17 System for computing the reduction factor for skewed piles.

$$f_{m4} = (0.8101)(0.8509)(0.9314)(0.7287)(0.9809) = 0.46$$

For the pile selected in the group, f_{ma} is the reduction factor to the values of p for the p-y curve. Pile 4 in the group significantly reduces the values of p for a single pile.

For each pile i in the group, the group reduction factor may be computed by the following equation:

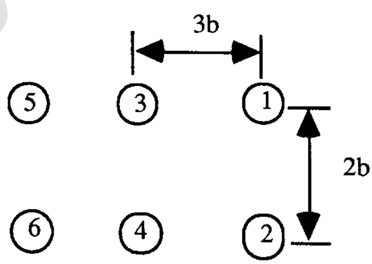

Figure 15.18 Pile group for example computations.

$$f_{mi} = \beta_{1i}\beta_{2i}\beta_{3i} \cdots \beta_{ji} \cdots m \neq i \tag{15.22}$$

Computation of the factor to reduce the values of p for the single pile to values for each pile in a group is tedious. Then the individual sets of p-y curves, perhaps all different, must be used in analyzing the behavior of the group under lateral loading. Such extensive computations require a properly written computer program.

15.6 EFFICIENCY OF PILES IN GROUPS UNDER AXIAL LOADING

15.6.1 Introduction

Most pile foundations consist not of a single pile, but of a group of piles for supporting superstructures. In a group of closely spaced piles, the axial capacity of the group is influenced by variations in the load-settlement behavior of individual piles because of pile–soil–pile interaction. The group effects of piles under axial loading, discussed in this chapter, will focus on proposals for determining the efficiency of the individual piles in the group.

The concept of group behavior is presented in Figure 15.19. Figure 15.19a shows a single pile and the possible downward movement of an imaginary surface at some distance below the groundline. As may be seen, that surface moves downward more at the wall of the pile than elsewhere, but movements do occur away from the wall.

Three piles spaced close together are shown in Figure 15.19b. The zones of influence overlap, so that the imaginary surface moves downward more for the group than for the single pile. The stresses in the soil around the center pile are larger than those for the single pile because of the transfer of stresses from the adjacent piles. Therefore, the designer must consider the ultimate capacity of a pile in a group as well as the settlement of the group.

The problem is complicated by the presence of the pile cap in two ways. First, if the cap is perfectly rigid and the axial loading is symmetrical, all of the piles will settle the same amount. However, if the cap is flexible, the settlement of the piles will be different. Second, if the cap rests on the ground surface, some of the axial load will be sustained by bearing pressure on the cap. Many authors have treated the problem of the distribution of the axial load to the piles and to the cap. However, conservatively, the assumption can be made that there can be settlement of the soil beneath the cap and that all of the load is taken by the piles. This above assumption is made in the discussion that follows.

Unlike the behavior of a group of piles under lateral loading, the behavior of a group under axial loading strongly depends on methods of installation, types of soils, and stress-induced settlement. The position of each pile in the group is less important than that of piles under lateral loading. A number of

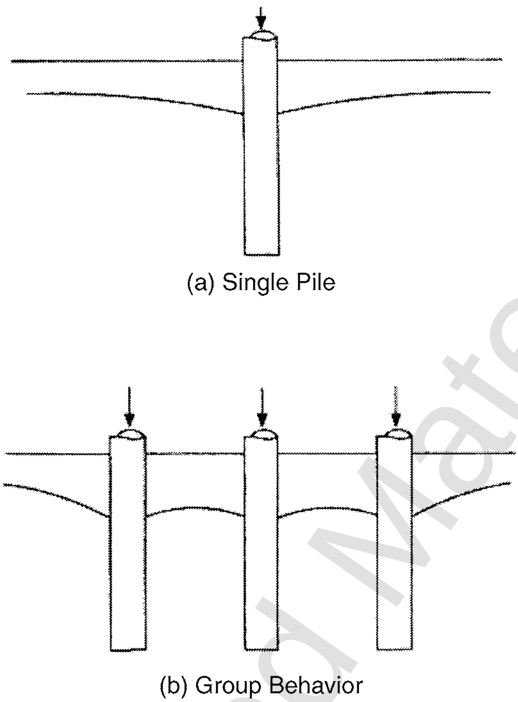

Figure 15.19 Group effects between closed-spaced piles.

investigators, such as Poulos and Davis (1980) and Focht and Koch (1973) have used the theory of elasticity to develop interaction recommendations. However, soils do not behave the same way in tension as in compression, and such theoretical results do not agree well with the results of experiments that have been conducted.

The concept of block failure (i.e., simultaneous failure of the piles and of the mass of soil within the pile group) is commonly used to calculate the ultimate capacity of a closed-spaced pile group. As shown in Figure 15.20, an imaginary block encompasses the pile group. The load carried by an imaginary block is the sum of the load carried by the base and friction on the perimeter of the block. The ultimate capacity developed by the block failure is compared with the sum of the ultimate capacity of individual piles in the group, and the smaller of these two values is selected as the load-carrying capacity of the pile group.

O'Neill (1983), in a prize-winning paper, presented a comprehensive summary of the efficiency of piles in a group. He reviewed the proposals that have been made for piles under axial loading and showed that piles in cohesive and cohesionless soils respond quite differently. Many investigations have been carried out to determine group efficiency under various soil conditions and pile spacings. A brief discussion of group efficiency in cohesionless and cohesive soils will now be presented for reference.

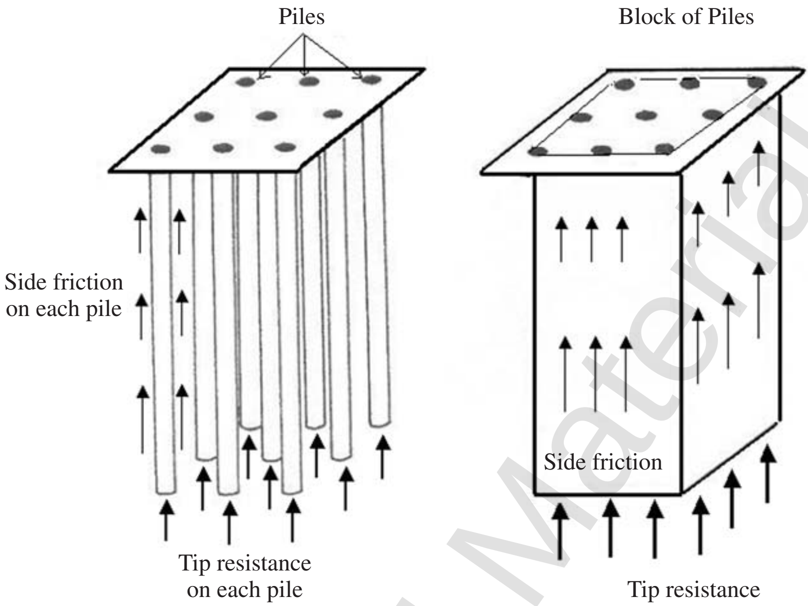

Figure 15.20 Block-failure model for closed-spaced piles.

15.6.2 Efficiency of Piles in a Group in Cohesionless Soils

The efficiency η of a pile in a group is defined formally by Eq. 15.23:

$$\eta = \frac{Q_g}{nQ_s} \tag{15.23}$$

where

η = number of piles,
Q_g = total capacity of the group, and
Q_s = capacity of a reference pile that is identical to a group pile but is isolated from the group.

Figure 15.21 shows the average efficiencies for driven piles. Theory predicts that the capacity of a pile in cohesionless soil is increased with an increase in the effective stress. Thus, the overlapping zones of stress at the base of a group of piles will cause an increase in end bearing. As shown in Figure 15.21, the average value of efficiency is slightly greater than unity. Also, the lateral compaction of the cohesionless soil during installation can cause an increase in effective stress along the sides of a driven pile (the shaft). Figure 15.21 shows that the efficiency of the shaft can range from slightly

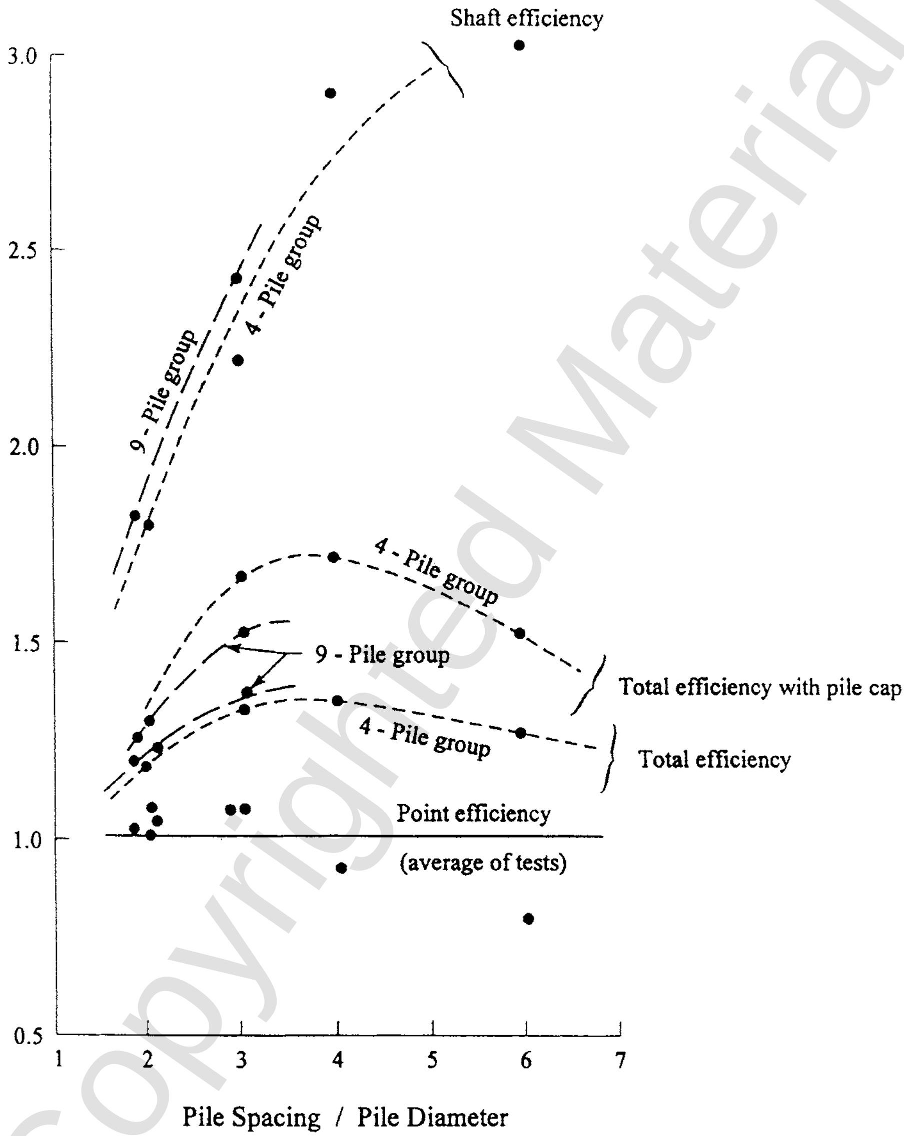

Figure 15.21 Group efficiency in cohesionless soils reported by Vesić (1969).

over 1.5 to almost 3.0. The figure shows that the overall efficiency of a group in cohesionless soils is well above 1.0.

While not shown in the figure, settlement frequently controls the capacity of piles in granular soils. Where settlement is critical, special study of the data from Vesić (1969) and from other authors is desirable.

O'Neill (1983) made a comprehensive study of the behavior of pile groups under axial loading. Figure 15.22 shows a compilation of the results of model tests for inserted piles (similar to those for driven piles). The trends in Figure 15.22 were described by O'Neill as follows: (1) η in loose sands always exceeds unity, with the highest values occurring at spacing-to-diameter ratios s/d of about 2, and in general, higher η occurs with increasing numbers of piles. Block failure (i.e., simultaneous failure of the piles and the mass of soil within the pile group) affects η in 4-pile groups only below s/d = 1.5 and in 9- to 16-pile groups only below s/d = 2. (2) η in dense sands may be either greater or less than unity, although the trend is toward $\eta > 1$ in groups of all sizes with s/d ranging from 2 to 4. Efficiency of less than unity is probably a result of dilatency and would not generally be expected in the field for other than bored or partially jetted piles, although theoretical studies of interference suggest η slightly below 1 at s/d > 4.

Conventional practice generally assigns a group efficiency value of 1 for driven piles in cohesionless soil unless the pile group is founded on dense soil of limited thickness underlain by a weak soil deposit. In such conditions, Meyerhof (1974) suggested that the efficiency value of the group should be based on the capacity of an equivalent base that punches through the dense sand in block failure.

15.6.3 Efficiency of Piles in a Group in Cohesive Soils

In general, piles in cohesive soils sustain load principally in side resistance or behave as "friction" piles. The load-carrying capacity of a group of friction piles in clay is the smaller of the following:

1. The sum of the failure loads of the individual piles or
2. The load carried by an imaginary block encompassing the group, where the loads is the sum of the load carried by the base and perimeter of the block.

In certain types of clay, particularly highly sensitive clay, the efficiency of closely spaced piles in a group is less than 1. However, there is insufficient data from testing of full-sized piles in the field to allow quantification of pile efficiency as a function of center-to-center spacing. Use of the imaginary block, described above, is the common way to investigate the efficiency of the group. The test results shown in Figure 15.23 were summarized by de Mello (1969) and show that failure of a pile group does not become pronounced until the pile spacing is less than two pile diameters.

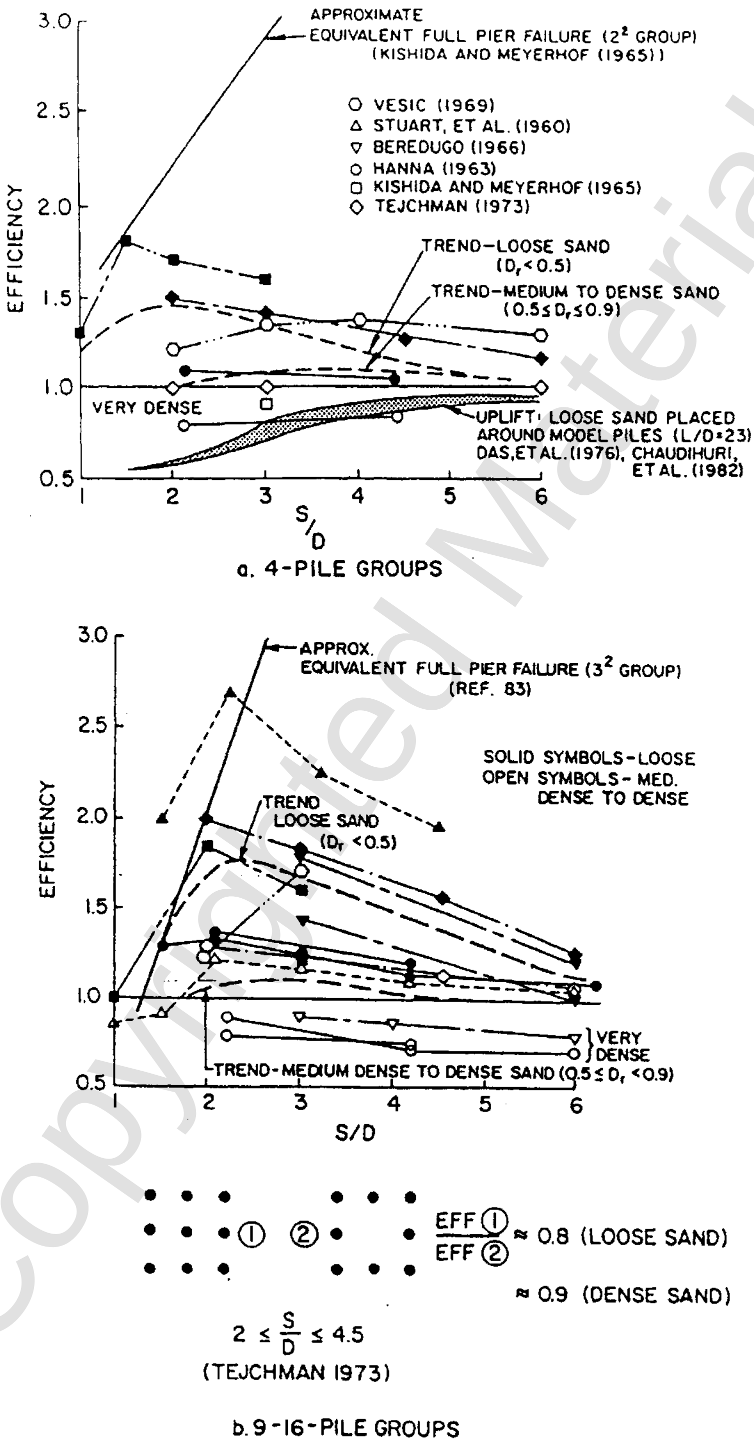

Figure 15.22 Group efficiency in cohesionless soils reported by O'Neill (1983).

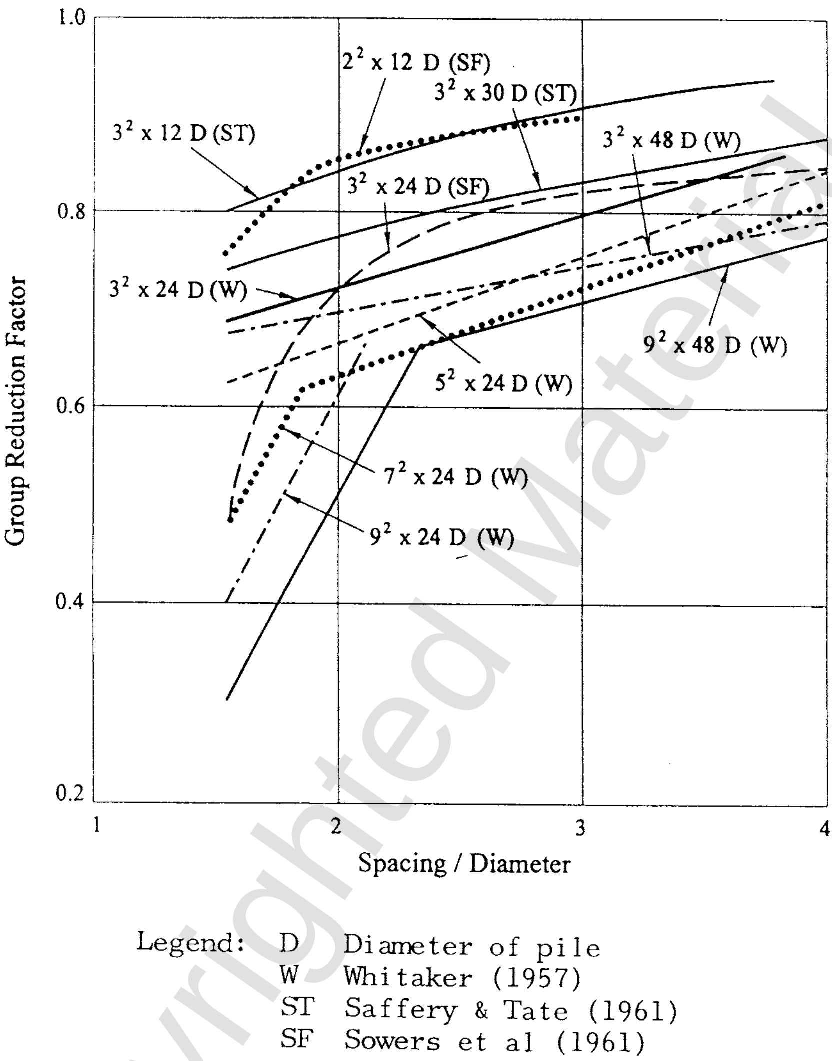

Figure 15.23 Group efficiency in cohesive soils reported by de Mello (1969).

O'Neill (1983) made studies of group efficiency in clay similar to those in sand. A compilation of the results of model tests of pile groups in clay is shown in Figure 15.24, except for the results reported by Matlock et al. (1980) where the test was in the field. Model tests in clay, in contrast to those in sand, always yield efficiencies less than 1, with a distinct trend toward block failure in square groups at values of s/d less than about 2. The group efficiency is higher in stiff clays than in soft clays.

O'Neill (1983) pointed out that the efficiencies are 1 or less for suspended caps and may be higher than 1 for caps in contact with the soil. However,

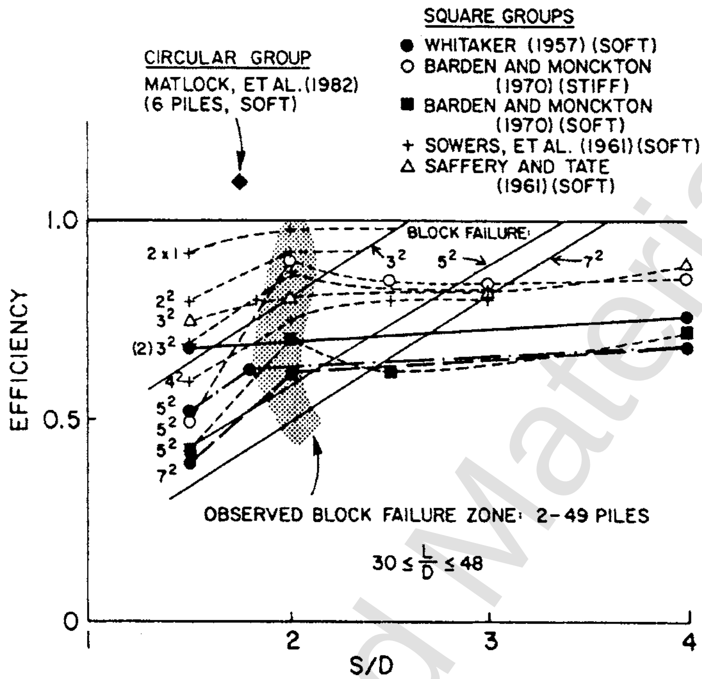

Figure 15.24 Group efficiency in cohesive soils reported by O'Neill (1983).

the possibility that the soil will settle eliminates the effectiveness of the cap. An important factor with respect to a group of piles in saturated clay is that the generation of porewater pressures during pile driving will create a large "bulb" of excess pore pressure around the group of piles. Thus, the dissipation of pore pressure around pile groups will be much slower than the dissipation around single piles, a fact that may not have been addressed in tests of full-scale piles that have been reported.

The settlement of a group of piles in saturated clay will be time-dependent and may be an overriding consideration with respect to the capacity of the group to sustain axial loading. The design of a group of piles in clay will depend on many factors, including site-specific conditions and the nature of the superstructure, as well as the center-to-center spacing of the piles.

15.6.4 Concluding Comments

The most reliable data on the efficiency of the piles in a group are derived from the results of full-scale tests. However, the behavior of pile groups under axial loading depends on many factors that can be investigated thoroughly only with a large number of carefully controlled tests, taking time into account. Such a program is beyond the capabilities of the agencies currently interested in the behavior of piles. As an example of the current limitations,

guidelines are unavailable for estimating the efficiency of groups of piles in layered soils. The data presented in this chapter are useful and present an introduction to the efficiency of piles in groups under axial loading, but they are not meant to provide specific information for design, even for the most routine problem. The judgment of the engineer should take into account the type of piles, construction methods, distribution of frictional and tip resistance, and dominant soil layers. As a concluding comment, the design of piles in groups under lateral and axial loading should be based on the concept of soil–structure interaction. Curves showing the transfer of lateral load (*p-y* curves), in side resistance (*t-z* curves), and in end bearing (*q-w* curves) can potentially be modified to account for the efficiency of the individual piles. Then both capacity and settlement can be computed with a rational model. This approach must await the performance of the requisite research.

PROBLEMS

P15.1. Make a tour of your neighborhood and look for places of where piles have been used in groups. Hint: in numerous instances, bridges and overpasses have been put on piles and the upper portions of the piles are exposed.

- **a.** Examine the upper portion of the piles where they are fastened to the pile cap and estimate, if possible, whether the designer meant the pile heads to be fixed against rotation or free to rotate.
- **b.** Look closely at the piles, made of reinforced concrete in many instances, and observe any possible overstressing, such as cracks in the concrete.
- **c.** Look closely as the soil where the piles are penetrating and look for cracks or openings next to the piles that indicate past deflection.
- **d.** Make a sketch of the pile group showing a plan of the pile heads and two elevations. Distances may be estimated. From your knowledge of the performance of groups of piles, discuss the selection of pile placement. If batter piles were used, is their placement exact, as measured by eye, or do they deviate from the planned position? Are some of the piles close enough together to require use of the technology to account for pile–soil–pile interaction?

P15.2. Select one or more of the references, go to the engineering library, and request the librarian to assist in finding it. Prepare a one-page summary.

P15.3. The two-dimensional problem of the pile group under lateral load resulted in the following solution:

$$\Delta v = 0.005579; \quad \Delta h = 0.025081; \quad \alpha_s = 0.000151$$

Use appropriate equations to compute the pile-head movements from the above values, compute pile-head forces, and check to determine if the group is in static equilibrium.

P15.4. Provide input for the problem of the retaining wall to perform a push-over analysis and solve for the loading that will cause failure by excessive movement or by excessive bending stress. Assume that the axial capacity of the pile is 200 k and the maximum bending stress is 36 ksi (note that using a multiplier of the loads of 2.5 yielded a computed maximum axial load of 99.5 k and a bending stress of 12.0 ksi). Also, the maximum stress occurs down the length of the pile rather than at the top.

P15.5. Assume that you wish to redesign the system for failure at a load factor of 3.0. List some of the modifications you would consider.